

Recording from two neurons: second order stimulus reconstruction from spike trains

N. M. Fernandes, B. D. L. Pinto, L. O. B. Almeida, J. F. W. Slaets and R. Köberle

Depart. de Física e Informática, Inst. de Física de São Carlos, USP, C. P. 369, CEP 13560-970, São Carlos-SP, Brasil, e-mail: rk@if.sc.usp.br

October 29, 2018

We study the reconstruction of visual stimuli from spike trains, representing the reconstructed stimulus by a Volterra series up to second order. We illustrate this procedure in a prominent example of spiking neurons, recording simultaneously from the two H1 neurons located in the lobula plate of the fly *Chrysomya megacephala*. The fly views two types of stimuli, corresponding to rotational and translational displacements. The second order reconstruction requires the manipulation of potentially very large matrices. Using a convenient set of basis functions to expand our variables in, we present a method, which avoids the computation and inversion of these matrices. This requires approximating the spike train 4-point functions by combinations of 2-point functions in a Gaussian-like fashion. The two parameters needed in this approximation can be computed using small matrices. In our test-case, this approximation does not reduce the quality of the reconstruction. The overall contribution to stimulus reconstruction of the second order kernels - measured by the mean squared error - is only about 5% of the first order contribution. Yet at specific stimulus-dependent instants, the addition of second order kernels represents an up to 100% improvement, but only for rotational stimuli.

1 Introduction

Living animals have to reconstruct a representation of the external world from the output of their sensory systems in order to correctly react to the demands of a rapidly varying environment. In many cases this sensory output is encoded into a sequence of identical action potentials, called spikes. If we represent the external world by a time-dependent stimulus function $s(t)$, the animal has to reconstruct $s(t)$ from a set of spikes. This decoding procedure therefore takes the set of spike trains and generates an estimate $s_e(t)$ of the stimulus, acting as an digital-to-analog converter.

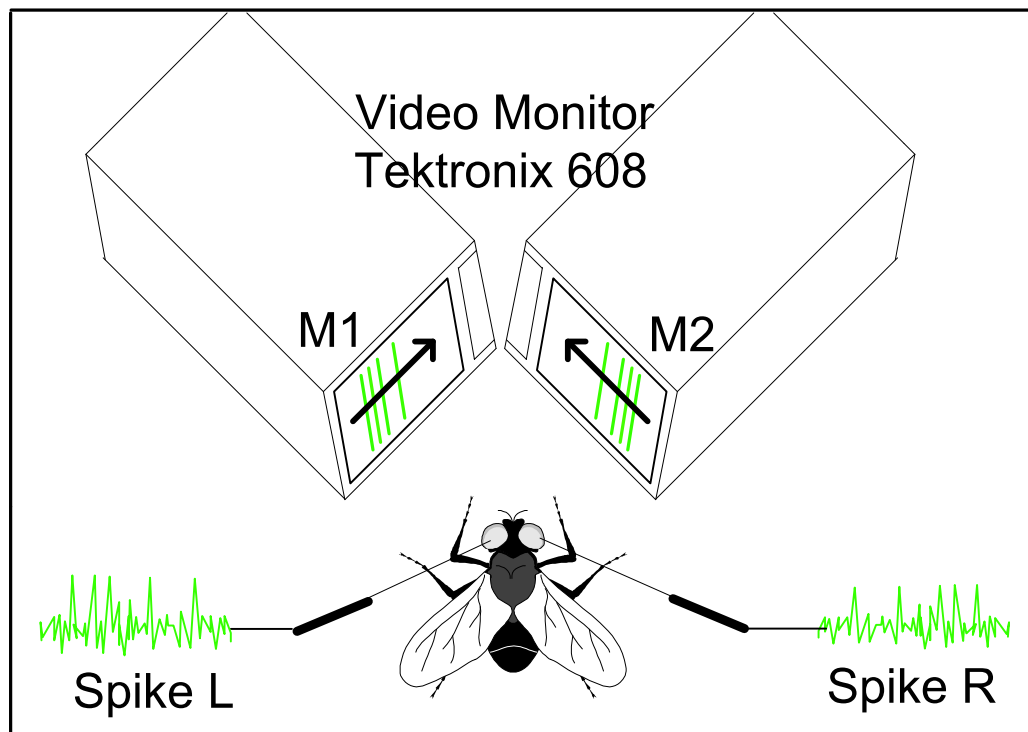


Figure 1: (Color online) Motion sensitivity of the two H1 neurons. Each eye sees a monitor displaying a rigidly moving bar pattern. The stimuli in this figure correspond to a translational motion in which both neurons are excited. Inverting the stimulus shown by monitor M1 would generate a rotational stimulus, which now inhibits the response of the left neuron. Electrodes record extracellularly from each H1.

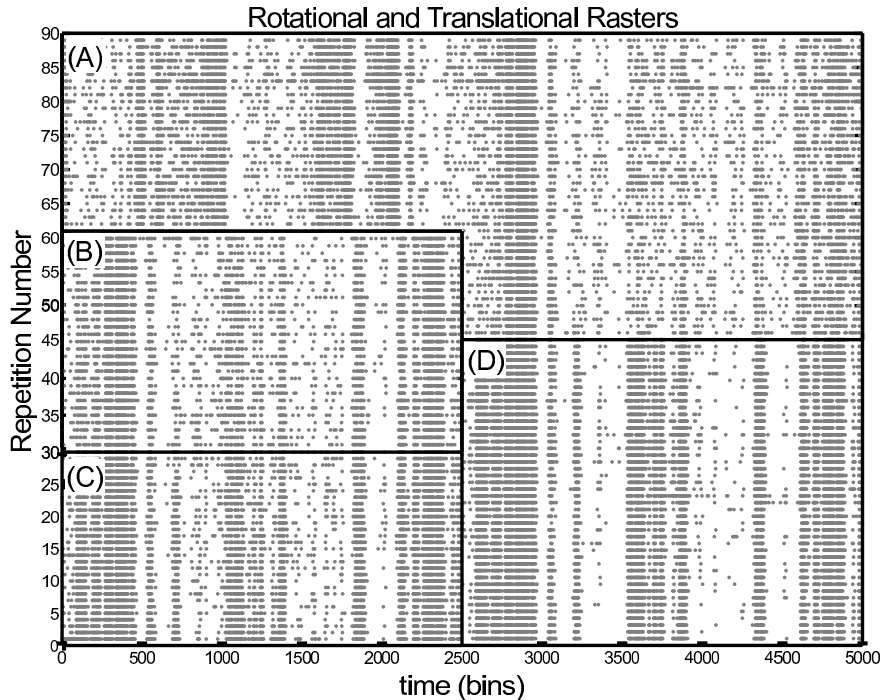


Figure 2: (Color online) Raster plot for the two H1 neurons, showing their complementary action under rotational and translational stimuli. The same time-dependent stimulus $s(t)$ is repeatedly shown to the fly, the horizontal time axis running from time zero to 5000 bins = 10 seconds and the vertical axis showing the repetition number. The responses of the neurons are shown as a raster, where each dot represents a spike. The right H1 sees a stimulus $s_r(t)$ and the left one sees $s_l(t)$. (A) Translational stimuli $s_r(t) = -s_l(t) = s(t)$, spikes from right H1. (B) Rotational stimuli $s_r(t) = s_l(t) = s(t)$, spikes from left H1. (C) Spikes from right H1, fly subjected to rotational sign reversed stimuli $s_r(t) = s_l(t) = -s(t)$, in order to simulate raster(B). (D) Translational stimuli $s_r(t) = -s_l(t) = s(t)$, spikes from left H1.

Here we study this decoding procedure in a prominent example of spiking neurons: the two H1 neurons of the fly *Chrysomya megacephala*. The fly has two compound eyes with their associated neural processing systems (Hausen, 1981), (Hausen, 1982), (Hausen, 1984). Each system is made up of several stages, one of them - the lobula plate - contains the H1 neuron. Each neuron

is sensitive to horizontal stimuli, being excited by back-to-front moving scenery as shown in Figure 1 and inhibited by oppositely moving stimuli. In a translational movement of the fly, the optical flux seen by the two eyes stimulates the two neurons about equally. Since their interaction is inhibitory, they effectively reduce each others output. In contrast, if the fly rotates around a vertical axis, say clockwise when looking down the axis, the left neuron is inhibited and the right one is excited. The left neuron's inhibition now ceases and the fly gets a strong signal from the right neuron, so that the two neurons function as an efficient rotational detector (Hausen, 1984). This can be seen in the raster-plots of Figure 2. Even when recording from only one H1, one can simulate the response of the contralateral H1. In fact, since the two H1 cells have mirror symmetric directional sensitivities, the sign flipped stimulus induces a response in the ipsilateral H1 typical for the contralateral H1 cell (Rieke, Warland, Steveninck, & Bialek, 1996). Comparing Figure 2 (B) and (C) we see this to be true to a very good approximation.

The second order reconstruction requires the computation of higher order spike-spike correlation functions and a subsequent matrix inversion. If one records from many neurons simultaneously, the size of these matrices may soon become prohibitively large. Here we present an efficient method to approximate these higher order correlation functions. It has far less computational costs, avoids large matrix inversions and gives excellent reconstruction results. We test the quality of our reconstructions under both rotational and translational stimuli.

2 Stimulus reconstruction from spike trains .

Suppose we want to reconstruct the stimulus from the response of a single H1 neuron. We represent this response as a spike train $\rho(t) = \sum_{i=1}^{N_s} \delta(t - t_i)$, which is a sum of delta functions at the spike times t_i . N_s is the total number of spikes generated by the neuron during the experiment.

The simplest reconstruction extracts the stimulus estimate via a linear transformation, see e.g. (Rieke et al., 1996),(Bialek, Rieke, Steveninck, & Warland, 1991),

$$s_e(t) = \int_{-\infty}^{\infty} k_1(\tau)\rho(t - \tau)d\tau, \quad (2.1)$$

with the kernel $k_1(t)$ to be determined.

For simplicity we effect an *acausal* reconstruction, i.e. we integrate from $-\infty$ to $+\infty$. Essentially the same results are obtained in a causal reconstruction. One way to implement causality proceeds to estimate the stimulus at time t , using as input the spike train up to time $t + t_0$. For the fly t_0 has to be \gtrsim to 30 milliseconds. In this case equation 2.1 would read: $s_e(t) = \int_{-t_0}^{\infty} k_1(\tau)\rho(t - \tau)d\tau$.

Equation 2.1 is the first term of a Volterra series (Martin, 2006):

$$s_e(t) = \int_{-\infty}^{\infty} k_1(\tau)\rho(t - \tau)d\tau + \int_{-\infty}^{\infty} k_2(\tau_1, \tau_2)\rho(t - \tau_1)\rho(t - \tau_2)d\tau_1d\tau_2 + \dots \quad (2.2)$$

There is no convergence proof for this expansion, but heuristically we may say that it should be a valid approximation, if the average number of spikes per correlation time τ_c

$$\eta = \langle r \rangle \tau_c \quad (2.3)$$

is small (Rieke et al., 1996). Here $\langle r \rangle$ is the mean spike rate and τ_c a typical signal correlation time. For small η each spike gives independent information about the stimulus. In our case $\eta \sim 0.6 - 0.8$, which is of the order of unity, so that higher order effects might be relevant.

In order to obtain the kernels k_1 and k_2 we choose to minimize the following functional - the χ^2 error -

$$\chi(k_1, k_2) = \left\langle \int dt [s(t) - s_e(t)]^2 \right\rangle. \quad (2.4)$$

The brackets stand for an ensemble average with respect to the distribution of all possible stimuli. In a long experiment we average over $N_w \sim 10^5$ time windows of size T_w . Typically $T_w \sim 100$ milliseconds - see section 7 for details.

Since the functional 2.4 is quadratic, the equations minimizing $\chi(k_1, k_2)$

$$\partial\chi/\partial k_j = 0, j = 1, 2 \quad (2.5)$$

are linear. E.g., if we keep only k_1 , using therefore equation 2.1, we get:

$$\tilde{k}_1(\omega) = \frac{\langle \tilde{s}(\omega) * \tilde{\rho}(\omega) \rangle}{\langle \tilde{\rho}(\omega) * \tilde{\rho}(\omega) \rangle}, \quad (2.6)$$

where Fourier transforms are defined as $\tilde{F}(\omega) = \int dt F(t)e^{i\omega t}$.

We may include the second order term k_2 , either as a correction to the first order reconstruction $s_1(t) = k_1 \star \rho(t)$ ¹, or one may solve the coupled

¹The symbol \star stands for a convolution as in equation 2.1.

system 2.5.

If we record simultaneously from left and right H1, we obtain two spike trains $\rho_1(t)$ and $\rho_2(t)$. The expansion equation 2.2 generalizes to

$$s_e(t) = K_1 \star \rho_1(t) + K_2 \star \rho_2(t) + \quad (2.7)$$

$$K_{11} \star \rho_1 \star \rho_1(t) + K_{12} \star \rho_1 \star \rho_2(t) + K_{22} \star \rho_2 \star \rho_2(t) + \dots$$

Here we have included the kernel K_{12} , which may be important to encode effects correlating ρ_1 and ρ_2 ².

To first order, keeping only K_1 and K_2 in the expansion 2.7, we get the following equations:

$$\tilde{\mathcal{S}}_a(\omega) = \sum_{b=1}^2 \tilde{K}_b(\omega) \tilde{R}_{ab}(\omega), \quad a = 1, 2 \quad (2.8)$$

where

$$\tilde{\mathcal{S}}_a(\omega) = \int dt dt' \langle s(t') \rho_a(t' - t) \rangle e^{i\omega t}. \quad (2.9)$$

and

$$R_{ab}(t_1, t_2) = \int dt \langle \rho_a(t - t_1) \rho_b(t - t_2) \rangle, \quad a, b = 1, 2. \quad (2.10)$$

Due to time-translation invariance $R_{ab}(t_1, t_2)$ is only a function of the difference: $R_{ab}(t_1, t_2) = R_{ab}(t_1 - t_2)$ and $\tilde{R}_{ab}(\omega) = \int dt R_{ab}(t) e^{i\omega t}$. Analogous properties hold for all the following correlation functions involving only $\rho(t)$.

The solution of equations 2.8 yields

$$K_a \tilde{\omega} = (L_a(\omega) R_{\hat{a}\hat{a}} - L_{\hat{a}}(\omega) R_{a\hat{a}}(\omega)) / \Delta, \quad a = 1, 2 \quad (2.11)$$

where

$$L_a(\omega) = \langle s(\omega) \rho_a^*(\omega) \rangle, \quad \Delta = R_{11} R_{22} - R_{12} R_{21} \quad (2.12)$$

and $\hat{a} = 3 - a$. We obtain the first order reconstruction as $s_1(t) = K_1 \star \rho_1(t) + K_2 \star \rho_2(t)$.

Since the second order contribution turns out to be small, we treat it as a perturbation to the first order reconstruction. We therefore expand $s_2(t) = s(t) - s_1(t)$ as:

$$s_2(t) = K_{11} \star \rho_1 \star \rho_1(t) + K_{12} \star \rho_1 \star \rho_2(t) + K_{22} \star \rho_2 \star \rho_2(t). \quad (2.13)$$

²Notice that we have not *orthogonalized* our expansion equation 2.2, so that there are $K_{11}(t_1, t_1)$ terms, which could have been absorbed in $K_1(t)$ and similarly for $K_2(t)$.

We now have to solve the following equations

$$\mathfrak{R}_{ab}^{(2)}(t_1, t_2) = \int dt_3 dt_4 \sum_{c,d=1}^2 K_{cd}(t_1, t_2) R_{abcd}^{(4)}(t_1, t_2, t_3, t_4), \quad (2.14)$$

where

$$\mathfrak{R}_{ab}^{(2)}(t_1, t_2) = \int dt \langle s_2(t) \rho_a(t - t_1) \rho_b(t - t_2) \rangle, \quad (2.15)$$

$$R_{abcd}^{(4)}(t_1, t_2, t_3, t_4) = \int dt \langle \rho_a(t - t_1) \rho_b(t - t_2) \rho_c(t - t_3) \rho_d(t - t_4) \rangle. \quad (2.16)$$

Although the system 2.14 is linear, the matrices to be inverted may be very large. We have to invert the matrix

$$\mathcal{M}_{AT}^{BT'} \equiv R_{abcd}^{(4)}(t_1, t_2, t_3, t_4), \quad (2.17)$$

where A, B are compound indices $A = [ab], B = [cd]$ labeling the neurons. $T = [t_1, t_2], T' = [t_3, t_4]$ are compound time indices of size N_w^2 . If we compute the correlation functions using a time window of $T_w = 128$ bins, with binsize = 2 milliseconds, then the size of $\mathcal{M}_{AN}^{BN'}$ is $\sim 128^4 \times 2^4 \sim 5 \times 10^9$. The matrices to be inverted may become prohibitively large, especially if we record from more than just two neurons³.

We therefore present below an approximation, which requires no large matrix inversion, at the price of using for $R_{abcd}^{(4)}$ a Gaussian-like representation with a small number of parameters.

3 Choosing a convenient set of functions _____

At this point it is convenient to use a complete set of basis functions $f_\mu(t)$, $\mu = 1, 2, \dots, n_f$ to expand our variables in. Depending on the case, it may be sufficient to use a small number n_f of functions $f_\mu(t)$ to get a useful representation. If n_f has only a slight dependence on window size T_w , this would allow one to increase T_w without further computational costs.

We expand our second order kernels as:

$$K_{ab}(t_1, t_2) = \sum_{\mu, \nu} f_\mu(t_1) f_\nu(t_2) \mathcal{D}_{\mu\nu}^{ab}. \quad (3.18)$$

³We may solve the above system in Fourier space and select a subset of frequencies in order to reduce the size of the system.

We also expand our correlation functions:

$$\mathcal{S}_{ab}^{(2)}(\tau_1, \tau_2) = \sum_{\mu, \nu} \mathcal{S}_{\mu\nu}^{ab} f_\mu(\tau_1) f_\nu(\tau_2) \quad (3.19)$$

and

$$\begin{aligned} R_{abcd}^{(4)}(\tau_1, \tau_2, \tau_3, \tau_4) = \\ \sum_{\alpha\beta\mu\nu} \mathcal{R}_{\alpha\beta\mu\nu}^{abcd} f_\alpha(\tau_1) f_\beta(\tau_2) f_\mu(\tau_3) f_\nu(\tau_4). \end{aligned} \quad (3.20)$$

Substituting the above expansions into equations 2.14, we get a set of linear equations to be solved for $\mathcal{D}_{\mu\nu}^{ab}$:

$$\mathcal{S}_{\mu\nu}^{ab} = \sum_{cd, \alpha\beta} \mathcal{R}_{\mu\nu\alpha\beta}^{abcd} \mathcal{D}_{\alpha\beta}^{cd} \quad (3.21)$$

Often a Fourier expansion is used, i.e. $f_\omega = e^{i\omega t}$. But we may exploit our liberty to choose the functions in a more profitable way. Since our 2-point function $R(t_1, t_2)$ is real, positive⁴ and symmetric in t_1, t_2 , it posses a complete set of eigenfunctions $h_\mu(t)$:

$$\int dt_2 R(t_1, t_2) h_\mu(t_2) = r_\mu h_\mu(t_1) \quad (3.22)$$

with eigenvalues $r_\mu, \mu = 1, \dots, N_w$. We now choose our functions as $f_\mu(t) = h_\mu(t)/\sqrt{r_\mu}$, which satisfy:

$$\int dt_1 dt_2 f_\mu(t_1) R(t_1, t_2) f_\nu(t_2) = \delta_{\mu\nu}. \quad (3.23)$$

This choice will avoid large matrix inversions, if at least part of our higher order correlation functions can be built from $R(t_1, t_2)$.

4 Gaussian-like (Gl) approximation for one neuron

In this section we present an approximation, which avoids the computation of the matrices equation 2.17. In order to avoid cluttering our expression

⁴In case this is not true, we just add a convenient constant.

with indices, we first present our approximation scheme for one neuron only, suppressing thus the indices a, b, \dots , all set to 1.

For our choice of functions to become useful, we have to express our 4-point functions $R^{(4)}$ in terms of $R(t) \equiv R_{11}(t_1 - t_2)$. If our spike-generating process were gaussian, we would have⁵:

$$R^{(4)}(1, 2, 3, 4) = R(1, 2)R(3, 4) + R(1, 3)R(2, 4) + R(1, 4)R(2, 3) - 2\langle\rho(t)\rangle^4, \quad (4.24)$$

where $\langle\rho(t)\rangle$ is just a constant, due to time-translation invariance.

This suggests the following approximation for $R^{(4)}$:

$$R^{(4)}(1, 2, 3, 4) = A [R(1, 2)R(3, 4) + R(1, 3)R(2, 4) + R(1, 4)R(2, 3)] - B, \quad (4.25)$$

where A and B are constants to be adjusted⁶. With this approximation $\mathcal{R}_{\mu\nu\alpha\beta}$ becomes

$$\mathcal{R}_{\mu\nu\alpha\beta} = A(\delta_{\mu\nu}\delta_{\alpha\beta} + 2\delta_{\mu\alpha}\delta_{\nu\beta}) - 2B n_\alpha n_\beta n_\mu n_\nu, \quad (4.26)$$

where $n_\mu = \int dt f_\mu(t) \langle\rho(t)\rangle$.

Using this expression and the shorthand $\mathcal{S}_{\mu\nu} \equiv \mathcal{S}_{\mu\nu}^{11}$ in equations 3.21, we get the following equations for the unknown coefficients $\mathcal{D}_{\mu\nu} \equiv \mathcal{D}_{\mu\nu}^{11}$

$$\mathcal{S}_{\mu\nu} = A[\text{tr}(\mathcal{D})\delta_{\mu\nu} + 2\mathcal{D}_{\mu\nu}] - 2BD_{nn} n_\nu n_\mu, \quad (4.27)$$

where $\text{tr}(\mathcal{D}) \equiv \sum_\mu \mathcal{D}_{\mu\mu}$ and $D_{nn} \equiv \sum_{\alpha\beta} n_\alpha \mathcal{D}_{\alpha\beta} n_\beta$ and the sums over μ, α, β run from 1 to N_w .

This system can now easily be solved by:

1. taking the trace over $\mu\nu$ to compute $\text{tr}(\mathcal{D}) \equiv D$ and
2. multiplying by n_μ, n_ν to compute D_{nn} .

We get

$$\mathcal{D}_{\mu\nu} = [\mathcal{S}_{\mu\nu}/A - D\delta_{\mu\nu} + 2Bn_\mu n_\nu D_{nn}]/2, \quad (4.28)$$

⁵We write $(1, 2, \dots)$ instead of (t_1, t_2, \dots)

⁶Any structure built only from $R(t_1, t_2)$ could be used for our method to work.

with

$$D = [2(1 - n_4)\mathcal{S}_{\mu\mu} + 2n_2 n_\mu \mathcal{S}_{\mu\nu} n_\nu] / \Delta, \quad (4.29)$$

$$D_{nn} = [(n + 2)n_\mu \mathcal{S}_{\mu\nu} n_\nu - \mathcal{S}_{\mu\mu} n_2] / \Delta, \quad (4.30)$$

where

$$\Delta = 2(T_w + 2)(1 - n_4) + 2n^2, n_2 \equiv \sum_{\mu} n_{\mu} n_{\mu}, n_4 \equiv (n_2)^2. \quad (4.31)$$

Although the spike generation process of the H1 neurons is not gaussian, the parametrization equation 4.25 is unexpectedly good, as we will see in the next section.

5 G1 approximation for two neurons ---

For two neurons we now have to decorate our formulas with the indices a, b, \dots . First we choose our functions $f_{\mu}(t)$ to diagonalize $R^{11}(t_1, t_2) = \langle \rho_1(t_1) \rho_2(t_2) \rangle$:

$$\int dt_1 dt_2 f_{\mu}(t_1) R^{11}(t_1, t_2) f_{\nu}(t_2) = \delta_{\mu\nu}. \quad (5.32)$$

To simplify our formulas, we assume symmetry between the two neurons: $R^{11} = R^{22}$.

The intermediate steps 1 and 2 above now increase, since we have to express several 4-point functions in terms of 2-point functions, not all of them being diagonal. Thus

$$\mathcal{R}_{\mu\nu\alpha\beta}^{1111} = [\delta_{\mu\nu}\delta_{\alpha\beta} + \delta_{\mu\alpha}\delta_{\nu\beta} + \delta_{\mu\beta}\delta_{\nu\alpha}]A_{1111} + B_{1111}^{\alpha\beta\mu\nu} \quad (5.33)$$

$$\mathcal{R}_{\mu\nu\alpha\beta}^{1112} = [\delta_{\mu\nu}R_{\alpha\beta}^{12} + \delta_{\mu\alpha}R_{\nu\beta}^{12} + \delta_{\nu\alpha}R_{\mu\beta}^{12}]A_{1112} + B_{1112}^{\alpha\beta\mu\nu} \quad (5.34)$$

$$\mathcal{R}_{\mu\nu\alpha\beta}^{1122} = [\delta_{\mu\nu}\delta_{\alpha\beta} + R_{\mu\alpha}^{12}R_{\nu\beta}^{12} + R_{\mu\beta}^{12}R_{\nu\alpha}^{12}]A_{1122} + B_{1122}^{\alpha\beta\mu\nu} \quad (5.35)$$

$$\mathcal{R}_{\mu\nu\alpha\beta}^{1222} = [R_{\mu\nu}^{12}\delta_{\alpha\beta} + R_{\mu\alpha}^{12}\delta_{\nu\beta} + R_{\mu\beta}^{12}\delta_{\nu\alpha}]A_{1222} + B_{1222}^{\alpha\beta\mu\nu} \quad (5.36)$$

$$\mathcal{R}_{\mu\nu\alpha\beta}^{2222} = [\delta_{\mu\nu}\delta_{\alpha\beta} + \delta_{\mu\alpha}\delta_{\nu\beta} + \delta_{\mu\beta}\delta_{\nu\alpha}]A_{2222} + B_{2222}^{\alpha\beta\mu\nu} \quad (5.37)$$

In the particular case of the two H1 neurons, we may further simplify this system, neglecting R^{12} . It's effect is very small indeed, since the action of the two neurons is complementary: an exciting stimulus for one neuron is inhibiting for the other⁷.

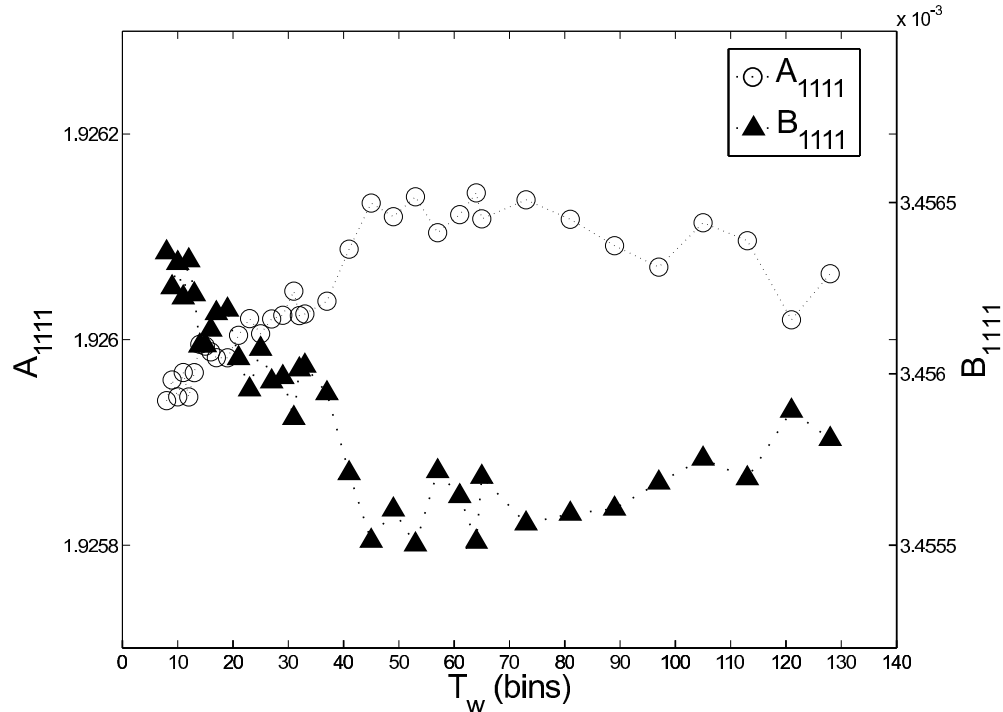


Figure 3: (Color online) Dependence of the parameter A_{1111} and B_{1111} on window size T_w . Similar behavior is found for the other parameters A and B . Notice that variations are on the 0.05% level.

The usefulness of our GI-approximation scheme depends on the quality of the 4-point functions obtained, which in turn hinges on the knowledge of the constants A_{abcd} and B_{abcd} . There would be no point, if this required the computation of 4-point functions in large window sizes and a fitting procedure using these windows - exactly what we wanted to avoid. We therefore fit the constants A_{abcd} and B_{abcd} for a sequence of window sizes, ranging from 10 to 128 bins. In this fit we used the first row of the matrix $\mathcal{R}_{[\alpha\beta][\mu\nu]}^{1111}$ ⁸. As can be seen in Figure 3, at least in the fly’s case, this dependence is on the 0.05% level and therefore completely negligible. The constants A_{abcd} and B_{abcd} can therefore be computed very fast in small windows. In Figure 4 we plot the

⁷The effect of R^{12} may be included perturbatively. In this case we have to solve a 5×5 system.

⁸We use here the same compound index notation as in equation 2.17.

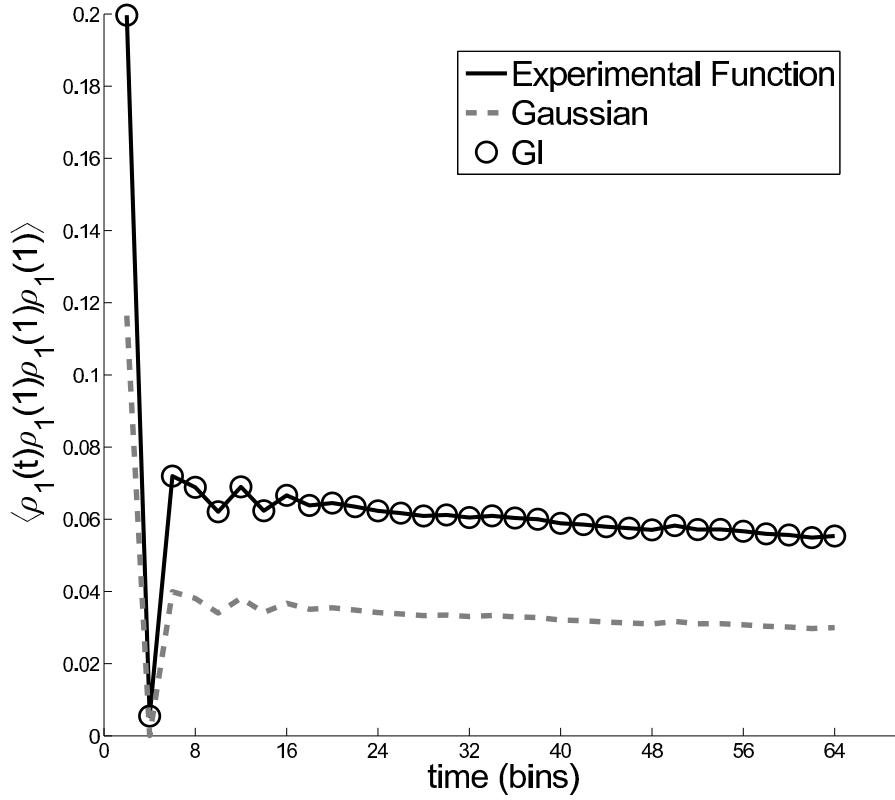


Figure 4: (Color online) 4-point functions and its GI approximation. We plot the first row of the matrix $R_{1111}^{(4)}$ for window-size $T_w = 64$ bins. The black continuous line is the experimental 4-point function. The gray dashed line is its Gaussian approximation without parametrization using equation 4.24. The black circles represent its GI approximation.

fits to the first row of the matrix $\mathcal{R}_{[\alpha\beta][\mu\nu]}^{1111}$ and its GI approximation. As advertised we obtain a perfect fit.

In Figures 5 we show the GI approximation for $R_{1111}^{(4)}$ matrix and its experimental version. Using the same parameters for the other entries of $\mathcal{R}_{[\alpha\beta][\mu\nu]}^{1111}$ and for $\mathcal{R}_{[\alpha\beta][\mu\nu]}^{2222}$ results in an error of about 20% larger.

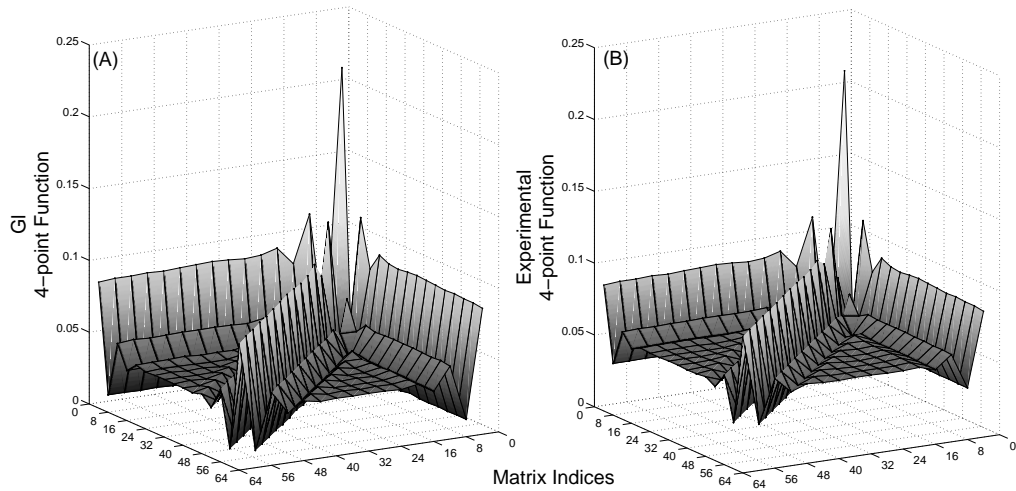


Figure 5: (Color online) (A) GI approximation and (B) experimental 4-point function for $R_{1111}^{(4)}$ for window-size $T_w = 64$ bins. We display the submatrix $\mathcal{M}_{1T}^{1T'}$ for $[T, T'] = [64, 64]$.

6 Reconstructing the fly's stimulus _____

To test the quality of our reconstructions, we use the data with $\eta \sim 0.8$, $\tau = 10$ msec and $\langle r \rangle \sim 80$ spikes/sec. We do not use the GI approximation in the following figures, since this would not make any difference. We also neglect K_{12} as illustrated in Figure 6, where we show $K_{12} \sim K_{22}/5$. Since the contribution of the second order terms is already small, K_{12} may be ignored. Our equations now decouple and we get two sets identical to equations 3.21, one for each eye.

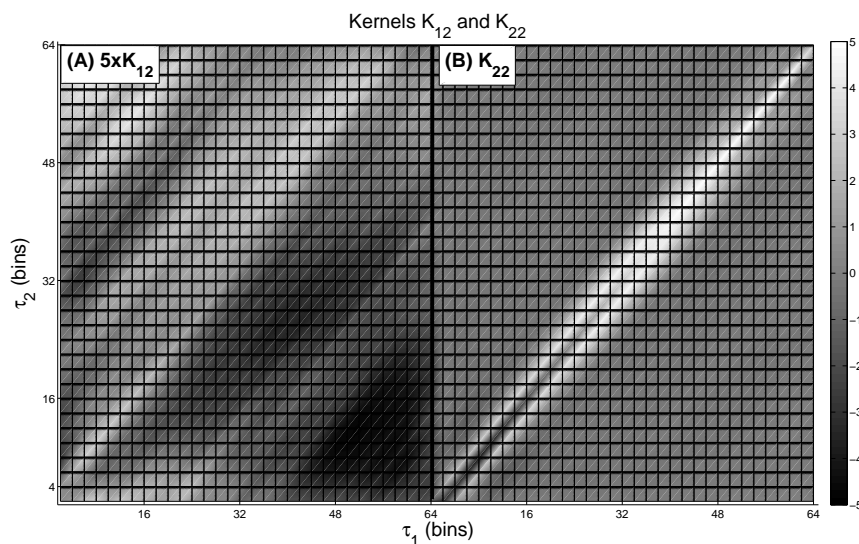


Figure 6: (Color online) Second order kernel $K_{22}(t, t)$ and upscaled version of $K_{12}(t, t)$ for $T_w = 64$. (A) $5 * K_{12}$, (B) K_{22} . Notice $K_{22}/K_{12} \sim 5$.

We select a representative sample, one second long, of the experiment, in order to give a visual display of the reconstruction. In figure 7 we show the first order reconstruction of the original stimulus using K_1 and K_2 and the second order reconstruction, where the effect of K_{11} and K_{22} is added. As we see, the reconstruction procedure is unable to reproduce the fast stimulus variations at the 2 milliseconds time scale. It is also clear that still higher order terms are not going to improve this deficiency. But the second order kernels always represent an improvement, although measured in terms of the total chi-squared error χ^2 of the whole experiment, it is only a 5% effect.

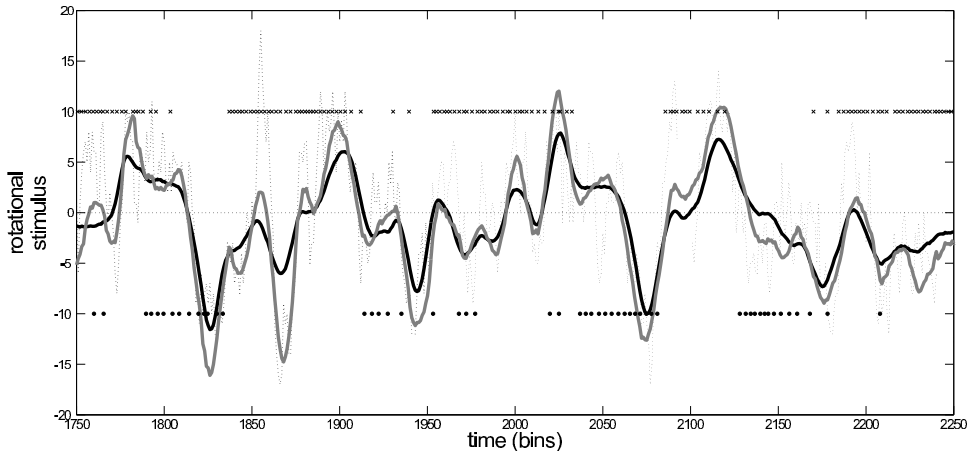


Figure 7: (Color online) Reconstructing the rotational stimulus with kernels K_1, K_2 and K_{11}, K_{22} , using the exact 4-point function. The black dashed line is the input stimulus to be reconstructed, the black continuous line represents the reconstruction using only K_1 and K_2 and the gray line represents the second order reconstruction. The \times and \bullet signs stand for the right and left spikes respectively.

For better visibility we smooth the stimulus with a Gaussian filter with a standard deviation of 10 milliseconds and repeat the reconstruction.. In figure 8 we show the result for rotational and translational stimuli. The improvement due to second order terms is plainly visible for rotational stimuli, but is much smaller for translational ones.

Although the improvement measured by the χ^2 is only 5%, the second order terms are a important at specific stimulus-dependent instants. We therefore measure local chi-squares:

$$\chi_1^2 \equiv \langle (s_1(t) - s(t))^2 \rangle \quad (6.38)$$

and

$$\chi_{12}^2 \equiv \langle (s_1(t) + s_2(t) - s(t))^2 \rangle \quad (6.39)$$

around instants T_2 , when χ_{12}^2 is at least as important as χ_1^2 . In figure 9 we plot the fraction of the stimulus-dependent instants vs. χ_{12}^2/χ_1^2 . Although this fraction vanishes as we require the importance of second order terms to increase, they still make a sizable contribution. With our amount of data,

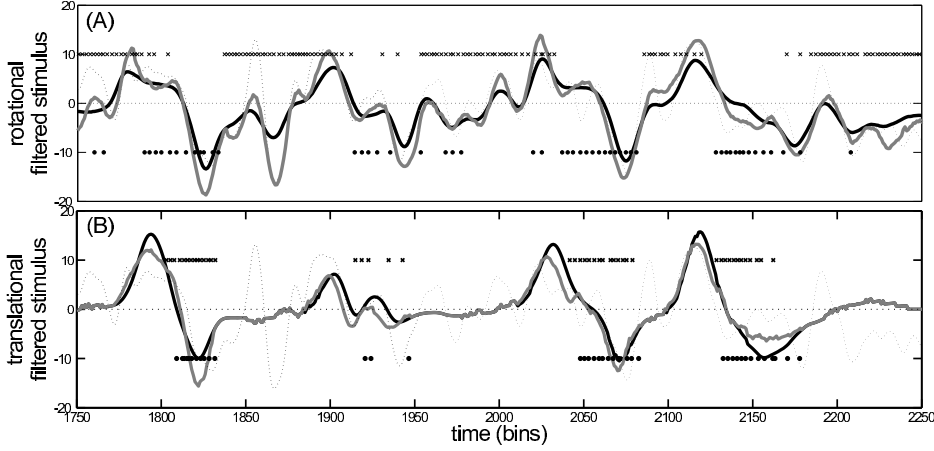


Figure 8: (Color online) Reconstructing filtered stimuli with kernels K_1, K_2 and K_{11}, K_{22} , using the exact 4-point function. Rotational (A) and translational stimulus (B). The black dashed line is the input stimulus, the black continuous line represents the reconstruction using only K_1 and K_2 and the gray line represents the second order reconstruction. The \times and \bullet signs represent the right and left spikes respectively.

we were unable to extract stimulus features, which might be relevant around T_2 .

Finally we follow (Rieke et al., 1996) and separate systematic from random errors, decomposing the estimate $\tilde{s}_e(\omega)$ into a frequency-dependent gain $g(\omega)$ and an effective noise $n_{eff}(\omega)$ referred to the input:

$$\tilde{s}_e(\omega) = g(\omega)(\tilde{s}(\omega) + n_{eff}(\omega)). \quad (6.40)$$

Around T_2 , we observe an overall improvement of 20% in $g(\omega)$.

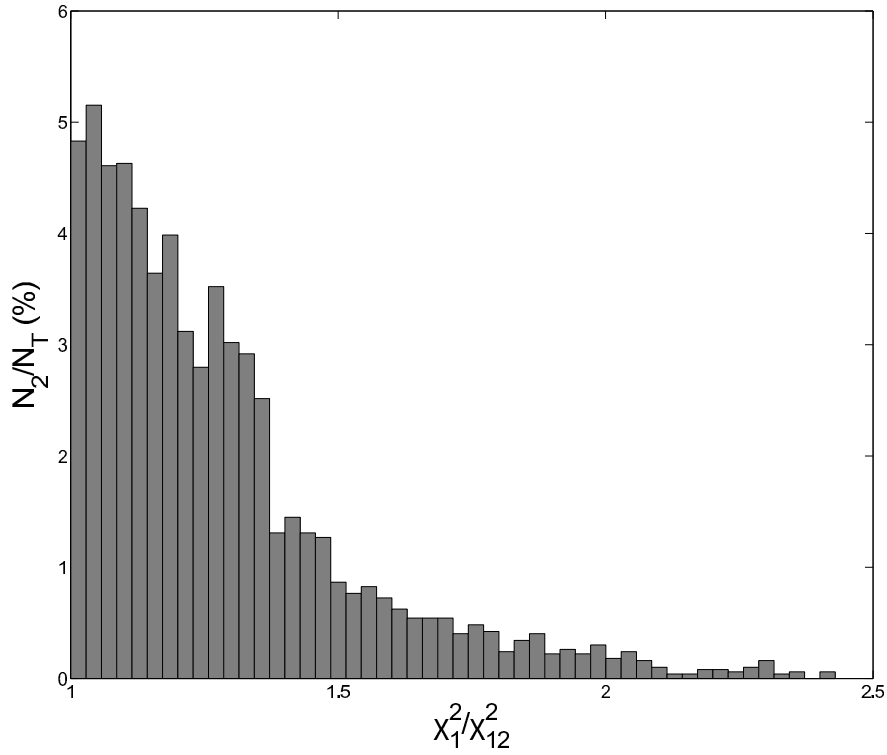


Figure 9: (Color online) N_2/N_T versus χ_1^2/χ_{12}^2 . We find the instants where χ_1^2/χ_{12}^2 assumes a particular value, when computed in windows of size 64 bins. N_2 is the number of these windows, whereas N_T is the duration of the experiment in bins divided by the window size.

7 Materials and Methods

Flies, immobilized with wax, viewed two Tektronix 608 Monitors M1, M2, one for each eye, from a distance of 12cm , as depicted in Figure 1. The monitors were horizontally centered, such that the mean spiking rates of the two neurons, averaged over several minutes, were equal. They were positioned, such that a straight line connecting the most sensitive spot of the compound eye to the monitor was perpendicular to the monitor’s screen. The light intensity corresponds roughly to that seen by a fly at dusk (Steveninck, Lewen, Strong, Köberle, & Bialek, 1997). The stimulus was a rigidly moving vertical bar pattern with horizontal velocity $v(t)$. We discretise time in bins of 2 milliseconds, which is roughly the refractory period of the H1 neurons. The fly therefore saw a new frame on the monitor every $\delta t = 2$ milliseconds, whose change in position δx was given by $\delta x(t) = v(t)\delta t$.

The velocity $v(t)$ was generated by an Ornstein-Uhlenbeck process with correlation times $\tau_c = 0, 5$ and 10 ms, i.e. the stimulus was taken from a Gaussian distribution with correlation function $C(t) = e^{-t/\tau_c}$. Experimental runs for each τ_c lasted 45 minutes, consisting of 20 seconds long segments. In each segment, in the first 10 seconds the same stimulus was shown, whereas in the next 10 seconds the fly saw different stimuli.

8 Summary

We analyze experiments on the fly’s visual system, where we record simultaneously from two H1 neurons. We present two types of stimuli: one simulating pure translational motion and the other pure rotational displacement. We use a Volterra expansion (Martin, 2006) up to second order to reconstruct the stimuli seen by the fly. For rotational stimuli, the second order contribution may be very important for special event times. The reconstruction method may require the handling of large matrices representing the spike train 4-point correlation functions $\langle \rho_a(t_1)\rho_b(t_2)\rho_c(t_3)\rho_d(t_4) \rangle$. We present a method, which avoids the computation and inversion of these potentially very large matrices. This requires approximating the 4-point correlation functions by combinations of 2-point functions in a Gaussian-like fashion depending on two parameters. The parameters can be computed using small window sizes. The reconstructions with and without approximations are virtually indistinguishable.

Acknowledgments

We thank I. Zuccoloto for her help with the experiments. The laboratory was partially funded by FAPESP grant 0203565-4. NMF was supported by a doctoral FAPESP fellowship. We thank Altera Corporation for their University program and Scilab for its excellent software.

References

- Bialek, W., Rieke, F., Steveninck, R. R. van, & Warland, D. (1991). Reading a neural code. *Science*, 252(5014), 1854-1857.
- Hausen, K. (1981). Monokulare und binokulare bewegungsauswertung in der lobula plate der fliege. *Verh. Dtsch. Zool. Ges.*, 49-70.
- Hausen, K. (1982). Motion sensitive interneurons in the optomotor system of the fly .2. the horizontal cells - receptive-field organization and response characteristics. *Biological Cybernetics*, 46(1), 67-79.
- Hausen, K. (1984). The lobula-complex of the fly: structure, function and significance in visual behaviour. In M. All (Ed.), *Photoreception and vision in invertebrates*.
- Martin, S. (2006). *The volterra and wiener theories of nonlinear systems*. New York: Krieger Publishing Co.
- Rieke, F., Warland, D., Steveninck, R. R. de Ruyter van, & Bialek, W. (1996). *Spikes-exploring the neural code*. Cambridge,USA: MIT Press.
- Steveninck, R. R. de Ruyter van, Lewen, G., Strong, S., Köberle, R., & Bialek, W. (1997). Reproducibility and variability in neural spike trains. *Science*, 275, 1805-1808.